

Competing effects of magnetic impurities in the anomalous Hall effect on the surface of a topological insulator

Ming-Xun Deng,¹ Wei Luo,¹ W. Y. Deng,¹ M. N. Chen,¹ L. Sheng,^{1,2,*} and D. Y. Xing^{1,2}

¹*National Laboratory of Solid State Microstructures and Department of Physics, Nanjing University, Nanjing 210093, China*

²*Collaborative Innovation Center of Advanced Microstructures, Nanjing University, Nanjing 210093, China*

(Received 27 September 2016; revised manuscript received 11 November 2016; published 5 December 2016)

We investigate the anomalous Hall effect (AHE) on the surface of a topological insulator induced by a finite concentration of magnetic impurities, and find topologically nontrivial and trivial mechanisms simultaneously contributing to the Hall conductivity. In the topologically nontrivial mechanism, the impurities gap the surface spectrum and result in a half-integer quantized intrinsic Hall conductivity in units e^2/h , while in the topologically trivial mechanism, the half-integer quantized plateau is modified by impurity-induced localized states via a gap-filling process. The nonmagnetic charge potential itself, though participating in the gap-filling process, cannot induce the AHE. In the presence of a finite magnetic potential, the charge potential would destroy the symmetric distribution of the Hall conductivity by redistributing the localized levels. More interestingly, the sign of the Hall conductivity is tunable by changing the strength of the charge potential.

DOI: [10.1103/PhysRevB.94.235116](https://doi.org/10.1103/PhysRevB.94.235116)

I. INTRODUCTION

Topological insulators (TIs) [1–3], possessing strong spin-orbit interactions and time-reversal symmetry (TRS), represent a novel quantum state of matter in condensed matter physics. TIs have a bulk band gap and gapless surface states protected by the TRS [4–6], being adiabatically distinct from ordinary insulators. The topological surface states (TSSs) are featured with a Dirac-like dispersion relation and a chiral spin structure due to spin-momentum interlocking [7–10]. Owing to their fundamental interest and promising applications in spintronics and topological quantum computation, manipulating the Dirac electronic properties or engineering the Dirac spectrum of the TI materials have been paid much attention recently [11–14]. Artificially creating an energy gap in the spectrum of the TSSs is one of the most promising pathways in the manipulation of the Dirac electrons [15–24], as the gap opening would result in multiple exotic phenomena, such as the recently observed quantum anomalous Hall effect (AHE) [25]. The AHE in conventional ferromagnetic metals [26], as a result of the interplay between the spin-orbit interaction and TRS breaking, has two distinct origins, intrinsic and extrinsic mechanisms. The intrinsic mechanism is dominated by the Berry curvature of the electron states below the Fermi energy, which can give rise to an integer or half-integer quantized Hall conductivity [27]. The extrinsic mechanism is an outcome of the scattering of the electrons near the Fermi energy by impurities [28–34].

Theoretically, doping magnetic impurities in TI materials would induce the AHE, due to broken TRS. Recently, theoretical investigations showed that magnetically doping the bulk of a TI material will lead to a gap opening for the TSSs [35,36], and a single magnetic impurity deposited on a TI surface with a finite spatial extent can gap the TSSs as well [37]. While no incipient gap was found for single pointlike magnetic impurity scattering [12], interestingly, for a finite concentration of pointlike magnetic impurities with

their spins ferromagnetically aligned [38], an energy gap can be generated. On the other hand, it was found that the energy gap could be filled rapidly by scattering off the strong nonmagnetic potential of impurities [18], and so the gap-opening effect may be unobservable from the density of states (DOS) of the TSSs in the strong potential scattering regime [24]. Compared to the DOS, the AHE is expected to be very sensitive to the energy gap, and can be experimentally probed by magneto-optical Faraday and Kerr effects [39,40]. Therefore, anomalous Hall conductivity may serve as an alternative measurable quantity for the experimental study of the properties of impurity-induced energy gap, especially when the scattering potential is strong. It is highly desirable to understand theoretically how the competing gap-opening and gap-filling processes caused by the magnetic impurities manifest themselves in the AHE of the TSSs.

In this paper, we study the AHE induced by a finite concentration of magnetic impurities deposited on a TI surface. We find that two mechanisms, topologically nontrivial and trivial mechanisms, relating to the gap-opening and gap-filling processes, contribute simultaneously to the Hall conductivity. In a topologically nontrivial mechanism, the magnetic impurities gap the Dirac spectrum, resembling a two-dimensional (2D) Dirac band in graphene or MoS₂ with spin-orbit coupling [29,31], which results in a half-integer quantized intrinsic Hall conductivity plateau in units e^2/h . In a topologically trivial mechanism, the extrinsic Hall conductivity due to impurity scattering, with signs opposite to the intrinsic Hall conductivity, develops peaks when the Fermi energy approaches the localized levels. The contributions from the two mechanisms separate well from each other in energy for weak magnetic impurity scattering. However, with increasing the strength of the magnetic potential, the trivial localized states would enter the gap gradually, making the two mechanisms compete with each other. As a result, the Hall conductivity plateau deviates from the half-integer quantized value in the strong impurity scattering regime. The charge potential itself, though taking part in the gap-filling process, cannot induce the AHE. For a finite magnetic potential, the charge potential will destroy the symmetric distribution of the

*shengli@nju.edu.cn

Hall conductivity due to the redistribution of localized levels. More interestingly, the sign of the Hall conductivity is tunable by adjusting the strength of the charge potential.

The rest of this paper is organized as follows. In the next section, we demonstrate the gap-opening and gap-filling processes caused by the magnetic impurities deposited on a TI surface. Then we study the magnetic-impurity-induced AHE on a TI surface in Sec. III. A brief summary is given in Sec. IV.

II. MAGNETIC-IMPURITY-INDUCED ENERGY GAP

Let us start from a continuum model of the TSSs with a low-energy effective Hamiltonian given by

$$H_0 = \sum_{\mathbf{k}} c_{\mathbf{k}}^\dagger [\hbar v_F (\mathbf{k} \times \hat{z}) \cdot \boldsymbol{\sigma} - \mu \sigma_0] c_{\mathbf{k}}, \quad (1)$$

where $c_{\mathbf{k}}^\dagger = (c_{\mathbf{k},\uparrow}^\dagger, c_{\mathbf{k},\downarrow}^\dagger)$ represents the electron creation operator at momentum $\mathbf{k} = (k_x, k_y)$, $\boldsymbol{\sigma}$ denotes the vector of the Pauli matrices for electron spin, and μ is the chemical potential. The eigenenergies of the Hamiltonian H_0 are $E_{\pm} = -\mu \pm \hbar v_F |\mathbf{k}|$, where the energy position of the Dirac point is determined by μ . The impurities are modeled by the Hamiltonian

$$H_{\text{imp}} = \sum_m \int c^\dagger(\mathbf{r}) V \delta(\mathbf{r} - \mathbf{r}_m) c(\mathbf{r}) d\mathbf{r}, \quad (2)$$

with $c^\dagger(\mathbf{r}) = \frac{1}{\sqrt{N}} \sum_{\mathbf{k}} c_{\mathbf{k}}^\dagger e^{-i\mathbf{k}\cdot\mathbf{r}}$ (N represents the number of the total states) and $V = U_0 \sigma_0 - J \mathbf{S} \cdot \boldsymbol{\sigma}$ being the scattering potential, which contains both a charge potential U_0 and a magnetic potential with \mathbf{S} as the spin of the impurity. The δ function in H_{imp} is used to approximate a spatially continuous scattering potential sharply peaked at the impurity sites. Since the quantum nature of the impurity spins is not crucial, we adopt the classical impurity model, in which the limits of large spin $|\mathbf{S}| \rightarrow \infty$ and weak hybridization $J \rightarrow 0$ are taken, but their product $J|\mathbf{S}|$ is kept to be finite [12,18].

For the TSSs to open an energy gap, we need to consider a finite concentration of magnetic impurities, as discussed in Ref. [12]. Under the perturbation of localized impurities, the configuration-averaged Matsubara Green's function of the TSSs reads

$$G(\mathbf{k}, i\omega_n) = G_0(\mathbf{k}, i\omega_n) + G_0(\mathbf{k}, i\omega_n) T(i\omega_n) G(\mathbf{k}, i\omega_n), \quad (3)$$

where $G_0(\mathbf{k}, i\omega_n) = [i\omega_n - H_0]^{-1}$ is the impurity-free Green's function, and $T(i\omega_n)$ is the T matrix, with ω_n as the Matsubara frequencies. The density of magnetic impurities, $\rho = \sum_m \int \delta(\mathbf{r} - \mathbf{r}_m) d\mathbf{r} / N$, is taken to be small, so that the T matrix can be evaluated within the first Born approximation [42], yielding $T(i\omega_n) = \rho [\sigma_0 - V \sum_{\mathbf{k}} G_0(\mathbf{k}, i\omega_n)]^{-1} V + O(\rho^2)$. The impurity-modified averaged Green's function, to first order in ρ , has the form $G(\mathbf{k}, i\omega_n) = [i\omega_n - H_0 - \Sigma(i\omega_n)]^{-1}$, where $\Sigma(i\omega_n)$ is the self-energy, given by

$$\Sigma(i\omega_n) = [\tilde{U}_0(i\omega_n) \sigma_0 - J \tilde{\mathbf{S}}(i\omega_n) \cdot \boldsymbol{\sigma}] \rho. \quad (4)$$

Here, $\tilde{U}_0(i\omega_n) = \frac{U_0 - g(i\omega_n) U_+ U_-}{[1 - g(i\omega_n) U_-][1 - g(i\omega_n) U_+]}$, $\tilde{\mathbf{S}}(i\omega_n) = \frac{\mathbf{S}}{[1 - g(i\omega_n) U_-][1 - g(i\omega_n) U_+]}$, $U_{\pm} = U_0 \pm J|\mathbf{S}|$, and $g(i\omega_n) = \frac{N(i\omega_n + \mu)}{4\pi(\hbar v_F)^2} \ln \frac{(i\omega_n + \mu)^2}{(i\omega_n + \mu)^2 - \Lambda^2}$, with Λ being a high-energy cutoff.

Expression (4) for the self-energy is valid for impurity spins ordered in an arbitrary direction. The self-energy is

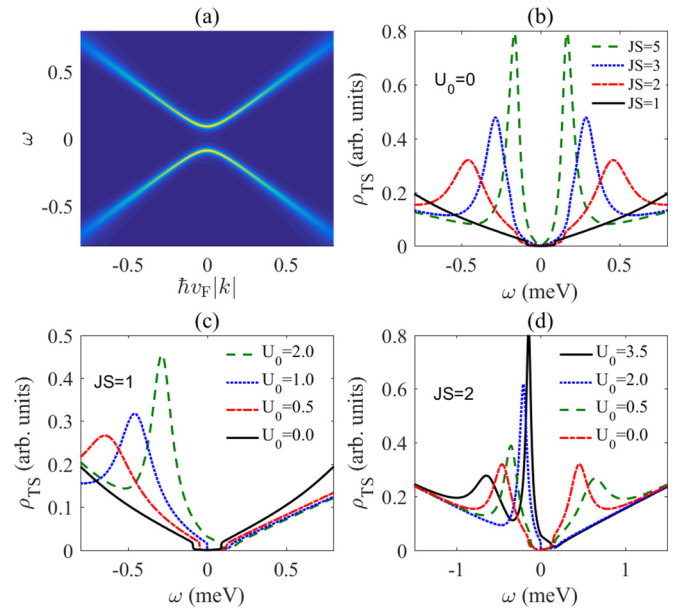


FIG. 1. (a) The low-energy band structure, given by $-\text{Im}\{\text{Tr}[G(\mathbf{k}, \omega^+)]\}/\pi$, for $U_0 = 0$ and $JS = 1$. (b)–(d) The DOS of the TSSs as a function of ω for some different choices of the parameters U_0 and JS . Here, $JS = J|\mathbf{S}_z|$, and the other parameters are taken to be $\mu = 0$, $\Lambda = 300$ meV (see, e.g., Ref. [8]) and $\rho = 0.1$ (the experimental value is about 0.08 measured in Ref. [41]). U_0 and JS are in units of meV.

an operator in the electron spin space, and plays the role of an effective potential energy. For a weak impurity scattering potential, i.e., $g(i\omega_n)U_{\pm}(i\omega_n) \ll 1$, the self-energy reduces to $\Sigma(i\omega_n) = (U_0 \sigma_0 - J \mathbf{S} \cdot \boldsymbol{\sigma}) \rho$, which is identical to the mean-field approximation of the impurity scattering potential. One can see that as long as the z component \mathbf{S}_z of the impurity spins is nonzero, an energy gap will appear around the Dirac point in the electron energy spectrum, with the gap size being proportional to $\rho J|\mathbf{S}_z|$. With increasing the strength of the magnetic scattering potential, the energy gap is expected to enlarge. However, as will be shown, some localized levels, which are determined by the poles of the Green's function, approach the Dirac point, leading to the gap-filling effect. Therefore, in the present approach, the gap-opening and gap-filling processes are treated on an equal footing, which are both described by the spin-dependent self-energy.

From the above discussion, we notice that no energy gap will appear, if all the spins of the magnetic impurities are confined in the x - y plane. We consider a favorable situation, where the spins of the magnetic impurities are aligned in the normal direction to the x - y plane. The self-energy then reduces to

$$\Sigma(i\omega_n) = [\lambda_+(i\omega_n) \sigma_0 + \lambda_-(i\omega_n) \sigma_z] \rho, \quad (5)$$

where $\lambda_{\pm}(z) = \frac{1}{2} \left[\frac{U_+}{1 - g(z) U_+} \pm \frac{U_-}{1 - g(z) U_-} \right]$.

In Fig. 1(a), we plot the low-energy band structure, given by $-\text{Im}\{\text{Tr}[G(\mathbf{k}, \omega^+)]\}/\pi$, with $\omega^{\pm} = \omega + i0^{\pm}$, for $U_0 = 0$ and $J|\mathbf{S}_z| = 1$. From Fig. 1(a), we see that for a moderate strength of the magnetic scattering potential, a well-defined energy gap will emerge. As indicated by Eq. (5), the size of the energy gap is defined by $\lambda_-(\omega) \rho$. It is proportional to $\rho J|\mathbf{S}_z|$ for a

weak magnetic scattering potential, which is very consistent with the observations in Ref. [41], because $\lambda_-(\omega)$ is dominated by U_\pm if $1/J|\mathbf{S}_z| \gg g(\omega)$. With increasing the strength of the magnetic scattering potential, the gap should get bigger, but the localized levels, determined by $1 \pm g(\omega)\rho J|\mathbf{S}_z| = 0$, approach the Dirac point. As a consequence, for a strong magnetic impurity scattering, the gap will become less noticeable in the DOS, because the impurity-induced localized states will fill the gap rapidly when they approach the Dirac point. The DOS of the TSSs is obtained as

$$\rho_{\text{TSS}}(\omega) = \text{Im} \left[\frac{\omega^+ + \mu - \lambda_+(\omega^+)\rho}{2\pi^2(\hbar v_{\text{F}})^2} \ln \frac{\mathcal{F}(\omega^+) - \Lambda^2}{\mathcal{F}(\omega^+)} \right], \quad (6)$$

where $\mathcal{F}(z) = [z + \mu - \lambda_+(z)\rho]^2 - [\lambda_-(z)\rho]^2$. In Fig. 1(b), we plot the calculated DOS as a function of ω , for several different values of $J|\mathbf{S}_z|$, demonstrating the gap-filling process by the localized levels.

The charge potential scattering would accelerate the gap-filling process by redistributing the localized levels and renormalizing the position of the Dirac point, as shown in Figs. 1(c) and 1(d). For a nonzero charge potential U_0 , the localized levels are determined by $1 \pm g(\omega)U_\pm = 0$. With increasing the charge potential U_0 , the localized level for $\omega < 0$ will approach the Dirac point, accompanied with an increasing and narrowing of the corresponding DOS peak. The localized level for $\omega > 0$ behaves in an opposite way. With increasing U_0 , it shifts away from the Dirac point, and the DOS peak vanishes gradually. As a result, the originally symmetric distribution of the localized levels is destroyed, as shown in Fig. 1(d). The localized level for $\omega > 0$ will entirely disappear if $U_0 \geq J|\mathbf{S}_z|$ (for $U_\pm > 0$), followed by another localized level emerging on the $\omega < 0$ side, as shown by the dark solid curve in Fig. 1(d). If U_0 changes sign, the behaviors of the localized levels for $\omega < 0$ and $\omega > 0$ will interchange. In the more complicated case, where the charge potential is randomly distributed with $\langle U_0 \rangle = 0$, the localized levels are expected to remain symmetrically distributed with respect to the Dirac point. We note that while it participates in the gap-filling process, the charge potential scattering alone cannot induce a gap for the TSSs, because $\lambda_-(\omega) = 0$ if $J|\mathbf{S}_z| = 0$.

In Ref. [24], Pieper *et al.* numerically investigated the effect of magnetic surface disorder on the TSSs. In their work, an inherent energy gap around the Dirac point was assumed to preexist and the magnetic surface disorder was modeled as a random Zeeman field. Though different in models and methods, their result is consistent with ours. For example, they also observed that the energy gap around the Dirac point in the DOS would become ambiguous for a strong magnetic potential. Therefore, alternative methods, other than the measurement of the DOS, are highly desirable to study the effects of impurities on the TSSs, especially when the impurity potential is strong.

III. MAGNETIC-IMPURITY-INDUCED AHE

The magnetically doped TI surface can host an interesting AHE, which will be studied in this section. The AHE has been extensively explored in quantum anomalous Hall systems [33], such as graphene [29,30], MoS₂ [31,32,34], and 2D electron gas [28]. Using the Streda-Smrcka [29,34] version of the Kubo

formula, one can divide the Hall conductivity into two different terms, $\sigma_{xy} = \sigma_{xy}^{\text{I}} + \sigma_{xy}^{\text{II}}$, with σ_{xy}^{I} and σ_{xy}^{II} corresponding to the contributions of the electrons at the Fermi level and below the Fermi level, respectively. It was found $\sigma_{xy}^{\text{I}} = 0$ and $\sigma_{xy}^{\text{II}} = -e^2/2h$ for the 2D Dirac band of a single spin of a single valley in graphene or MoS₂ in the insulating regime, and $\sigma_{xy}^{\text{I}} = -\frac{\Delta}{2\sqrt{(vk_{\text{F}})^2 + \Delta^2}} \frac{e^2}{h}$ and $\sigma_{xy}^{\text{II}} = 0$ in the metallic regime.

The Kubo-Streda formula can be expressed in terms of Green's functions as

$$\sigma_{\alpha\beta}^{\text{I}} = -\frac{e^2\hbar}{4\pi} \int d\epsilon \frac{df(\epsilon)}{d\epsilon} \text{Tr} \{ v_\alpha [G^R(\epsilon) - G^A(\epsilon)] v_\beta \times G^A(\epsilon) - v_\alpha G^R(\epsilon) v_\beta [G^R(\epsilon) - G^A(\epsilon)] \}, \quad (7)$$

and σ_{xy}^{II} is easy to find in Refs. [29,34]. Here, $v_{\alpha/\beta} = \partial H/\hbar\partial k_{\alpha/\beta}$ is the velocity operator and $G^{R/A}(\epsilon)$ is the retarded (advanced) Green's function. For convenience, we rewrite the impurity-modified Matsubara Green's function for the TSSs as $G(\mathbf{k}, i\omega_n) = \sum_{\eta=\pm} \frac{1}{i\omega_n - \xi_\eta} (\frac{1}{2}\sigma_0 + \eta P)$, with $\xi_\pm = -\mu + \lambda_+(i\omega_n)\rho \pm \sqrt{(\hbar v_{\text{F}}|\mathbf{k}|)^2 + [\lambda_-(i\omega_n)\rho]^2}$ and

$$P = \frac{1}{\xi_+ - \xi_-} \begin{pmatrix} \lambda_-(i\omega_n)\rho & \hbar v_{\text{F}}(k_y + ik_x) \\ \hbar v_{\text{F}}(k_y - ik_x) & -\lambda_-(i\omega_n)\rho \end{pmatrix}. \quad (8)$$

Employing Eqs. (7) and (8) and the relation $G^{R/A}(\epsilon) = G(\mathbf{k}, \epsilon^\pm)$, we derive the extrinsic and intrinsic Hall conductivities σ_{xy}^{I} and σ_{xy}^{II} for the magnetically doped TI surface to be

$$\sigma_{xy}^{\text{I}} = -\frac{e^2}{h} \frac{\pi - \phi}{\pi} \text{Im} \left[\frac{E_{\text{F}}^- + \mu - \lambda_+(E_{\text{F}}^-)\rho}{|\mathcal{F}(E_{\text{F}}^-)| \sin \phi} \lambda_-(E_{\text{F}}^+)\rho \right] \quad (9)$$

and

$$\sigma_{xy}^{\text{II}} = -\frac{e^2}{h} \int \frac{d\epsilon}{\pi} f(\epsilon) \text{Im} \left[\frac{1 - 2\lambda_+(\epsilon^-)\tilde{\epsilon}\partial_\epsilon g(\epsilon^-)}{\mathcal{F}(\epsilon^-)} \lambda_-(\epsilon^-)\rho \right], \quad (10)$$

where $\tilde{\epsilon} = \epsilon + i0^- + \mu - \lambda_+(\epsilon^-)\rho$, E_{F} is the Fermi energy, and ϕ is the argument of $\mathcal{F}(E_{\text{F}}^-)$.

As expected, the Hall conductivity is generated by an effective Zeeman-like field, namely, $\lambda_-(\epsilon^-)\rho$, produced by the collective effect of a finite concentration of magnetic impurities. The magnetic-impurity-induced effective Zeeman-like field is distinct from the intrinsic mass term induced by the spin-orbit interaction for the 2D Dirac band in graphene and MoS₂ [29,31], because the energy-dependent Zeeman-like term here, $\lambda_-(\epsilon^-)\rho$, determined by the impurity density ρ and the scattering potentials U_\pm , contains both the topologically nontrivial and trivial contributions.

In the topologically nontrivial mechanism, the magnetic impurities gap the TSSs, and result in a half-integer quantized intrinsic Hall conductivity plateau in units of e^2/h ($\sigma_{xy}^{\text{I}} = 0$ and $\sigma_{xy}^{\text{II}} = e^2/2h$), when the Fermi level is within the energy gap, as can be seen from Figs. 2(a) and 2(b). To see more clearly the contribution from the topologically nontrivial mechanism, we note that the function $g(\epsilon^-)$ accounts for the impurity scattering effect, and its key role is to generate localized electron states, as has been discussed in Sec. II, relating to the topologically trivial mechanism. The intrinsic Hall conductivity is mainly determined by the topological structure

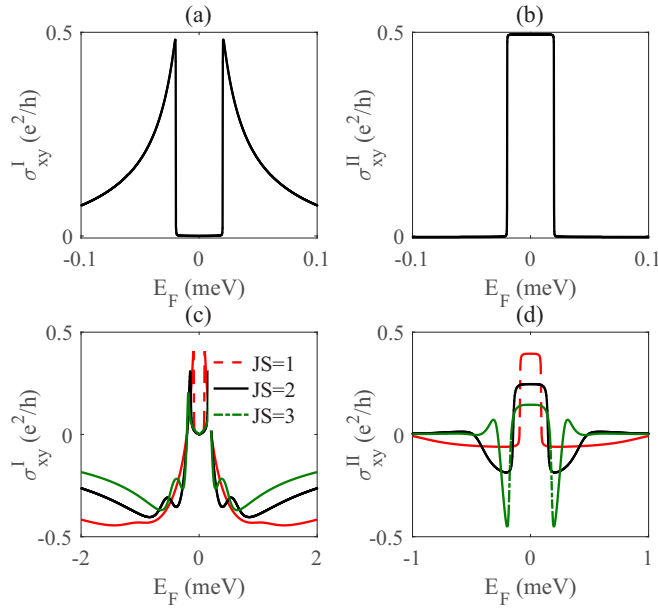


FIG. 2. Hall conductivities σ_{xy}^I and σ_{xy}^{II} vs E_F for $JS = 0.2$ in (a) and (b), and varied JS in (c) and (d). Here, $U_0 = 0$, and the other parameters are chosen to be the same as in Fig. 1.

of the valence band, and is insensitive to $g(\epsilon^-)$. Therefore, we can reduce Eqs. (9) and (10) by setting $g(\epsilon^-) = 0$, and find the intrinsic Hall conductivity to be

$$\sigma_{xy}^{I,int} = \frac{e^2}{h} \frac{\rho J |\mathbf{S}_z|}{4} \frac{\theta(E_F + \mu - \rho U_+) - \theta(\rho U_- - E_F - \mu)}{E_F + \mu - \rho U_0} \quad (11)$$

and

$$\sigma_{xy}^{II,int} = \frac{e^2}{h} \frac{f(-\mu + \rho U_-) - f(-\mu + \rho U_+)}{2}, \quad (12)$$

which is obviously half-integer quantized for the Fermi level within the energy gap.

For a weak magnetic impurity scattering, the gap-filling process is suppressed, and the contributions from the topologically nontrivial and trivial mechanisms separate well from each other in energy. As a result, the plateau of the Hall conductivity resides at the half-integer quantized value. With increasing $\rho J |\mathbf{S}_z|$, the Hall conductivity plateau will deviate from the half-integer quantized value, since the trivial localized levels enter the gap gradually. The plateau of σ_{xy}^{II} , as shown in Fig. 2(d), reduces its height due to the competition between the topologically nontrivial and trivial mechanisms. In fact, the gap cannot be fully filled by the localized levels, since the Dirac point is decoupled to the classical impurities, and the impurity-induced bound states cannot cross the Dirac point. As a result, the gap-filling process by the localized levels does not destroy the topological nature of the system, and the Hall conductivity plateau does not vanish completely during the gap-filling process.

In the metallic regime for a Fermi level out of the energy gap, the property of the Hall conductivity is dominated by the contribution of the electrons at the Fermi surface, including the intrinsic and extrinsic contributions. The intrinsic contribution, i.e., Eqs. (11) and (12), is similar to that for the 2D Dirac band

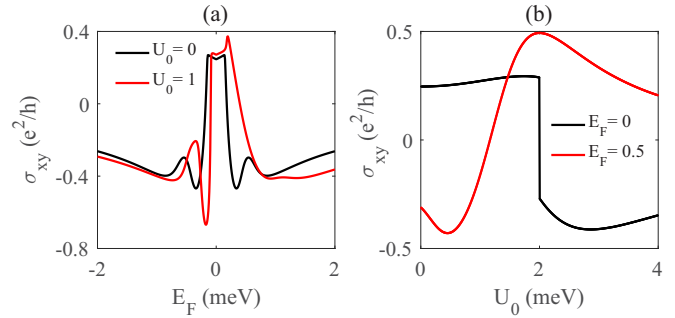


FIG. 3. Hall conductivity $\sigma_{xy} = \sigma_{xy}^I + \sigma_{xy}^{II}$ vs E_F in (a), and vs U_0 in (b), for $J|\mathbf{S}_z| = 2$. The other parameters are the same as in Fig. 1.

of a single spin and a single valley in graphene or MoS₂ with an intrinsic gap, where $\sigma_{xy}^{int} = \frac{e^2}{h} \frac{\Delta}{2|E_F|}$ and it decays monotonously to zero without changing its sign, when the Fermi energy shifts away from the energy gap. However, due to the topological trivial mechanism, the impurity-scattering-induced extrinsic Hall conductivity can overwhelm the intrinsic one, as shown in Figs. 2(c) and 2(d). The impurity scattering processes mainly occur around the localized levels, where the Hall conductivity may change its sign and develop peaks. It is quite different from a clean system in that, besides σ_{xy}^I , σ_{xy}^{II} can also contribute to the extrinsic Hall conductivity. Similar to σ_{xy}^I , σ_{xy}^{II} first reaches a negative maximum around the localized levels and then decays to zero as the Fermi level shifts away from the gap. As we increase the magnetic potential, the peaks of the extrinsic Hall conductivity will approach the energy gap, and overlap the intrinsic Hall conductivity plateau.

In addition to the main peaks in σ_{xy}^I , one may notice from Fig. 2(c) that two other small peaks emerge, decorating the main peaks. In fact, to the first order in ρ , we can obtain

$$\sigma_{xy}^{I,ext} = \frac{e^2}{h} \frac{\pi - \phi}{2\pi} \frac{\text{Im}[\lambda_-(\epsilon^+)]}{\text{Im}[\lambda_+(\epsilon^-)]}. \quad (13)$$

From this formula, one can find that the main peaks originate from $\text{Im}[\lambda_-(\epsilon^+)]/\text{Im}[\lambda_+(\epsilon^-)]$, and the small peaks are attributable to ϕ .

A nonmagnetic charge potential alone cannot induce the AHE, because if $J|\mathbf{S}_z| = 0$, $\lambda_-(\epsilon) = 0$, and both the intrinsic and extrinsic Hall conductivities vanish, as indicated by Eqs. (9) and (10). In the presence of a finite magnetic impurity potential, the charge potential can destroy the symmetrical distribution of the Hall conductivity through redistributing the localized levels, as shown in Fig. 3(a). More interestingly, from Fig. 3(b), we see that the sign of the Hall conductivity is tunable by the strength of the charge potential U_0 .

In the above discussion, $JS > 0$ is assumed. The generalization of the conclusion to $JS < 0$ is straightforward. The effective Zeeman-like field $\lambda_-(\epsilon^-)\rho$ is dependent on the exchange coupling JS . When changing the sign of JS , the effective Zeeman-like field changes its sign, and as a result, the anomalous Hall conductivity will change sign as well.

Our calculation is done in a 2D bulk. For a finite ribbon, one would expect edge states to carry the Hall conductivity. A finite ribbon has two surfaces, and contributions to the Hall conductivity from the two surfaces are additive, giving rise

to an integer-quantized Hall conductivity. If the total Hall conductivity is e^2/h , then there will exist one chiral edge state at an edge of the ribbon, which is jointly possessed by the two surfaces. The truncation of the two surface bulk bands only corresponds to one band of the edge states, similar to the truncation of K and K' valleys in graphene [29]. In our paper, the classical impurity model is employed. In a more complicated case, e.g., for quantum impurities, the Ruderman-Kittel-Kasuya-Yosida (RKKY) interactions are shown to be strongly nonuniform [41], and how these interactions affect the gap-filling and gap-opening effects of the impurities is still an open question.

IV. SUMMARY

The anomalous Hall effect induced by magnetic impurities on a TI surface has been studied. We find both topologically nontrivial and trivial mechanisms simultaneously contribute to the Hall conductivity. The former gaps the surface spectrum,

resulting in a half-integer quantized intrinsic Hall conductivity in units e^2/h in the insulating regime, and the latter modifies the half-integer quantized plateau of the Hall conductivity by filling the gap with trivial localized states. The charge potential scattering itself, though participating in the gap-filling processes, cannot induce the AHE, but it destroys the symmetric distribution of the Hall conductivity by redistributing the localized levels and can modify the sign of the Hall conductivity.

ACKNOWLEDGMENTS

This work was supported by the State Key Program for Basic Researches of China under Grants No. 2015CB921202, and No. 2014CB921103 (L.S.), the National Natural Science Foundation of China under Grants No. 11674160, and No. 11225420 (L.S.), and a project funded by the PAPD of Jiangsu Higher Education Institutions.

-
- [1] M. Z. Hasan and C. L. Kane, *Rev. Mod. Phys.* **82**, 3045 (2010).
 [2] X.-L. Qi and S.-C. Zhang, *Rev. Mod. Phys.* **83**, 1057 (2011).
 [3] J. E. Moore, *Nature (London)* **464**, 194 (2010).
 [4] L. Fu, C. L. Kane, and E. J. Mele, *Phys. Rev. Lett.* **98**, 106803 (2007).
 [5] J. E. Moore and L. Balents, *Phys. Rev. B* **75**, 121306 (2007).
 [6] J. C. Y. Teo, L. Fu, and C. L. Kane, *Phys. Rev. B* **78**, 045426 (2008).
 [7] D. Hsieh, D. Qian, L. Wray, Y. Xia, Y. S. Hor, R. J. Cava, and M. Z. Hasan, *Nature (London)* **452**, 970 (2008).
 [8] H. Zhang, C.-X. Liu, X.-L. Qi, X. Dai, Z. Fang, and S.-C. Zhang, *Nat. Phys.* **5**, 438 (2009).
 [9] Z.-H. Pan, E. Vescovo, A. V. Fedorov, D. Gardner, Y. S. Lee, S. Chu, G. D. Gu, and T. Valla, *Phys. Rev. Lett.* **106**, 257004 (2011).
 [10] T. Valla, Z.-H. Pan, D. Gardner, Y. S. Lee, and S. Chu, *Phys. Rev. Lett.* **108**, 117601 (2012).
 [11] D. Soriano, F. Ortmann, and S. Roche, *Phys. Rev. Lett.* **109**, 266805 (2012).
 [12] J. Fransson, A. M. Black-Schaffer, and A. V. Balatsky, *Phys. Rev. B* **90**, 241409 (2014).
 [13] R.-Q. Wang, L. Sheng, M. Yang, B. Wang, and D. Y. Xing, *Phys. Rev. B* **91**, 245409 (2015).
 [14] M.-X. Deng, R.-Q. Wang, W. Luo, L. Sheng, B. G. Wang, and D. Y. Xing, *New J. Phys.* **18**, 093040 (2016).
 [15] Y. L. Chen, J.-H. Chu, J. G. Analytis, Z. K. Liu, K. Igarashi, H.-H. Kuo, X. L. Qi, S. K. Mo, R. G. Moore, D. H. Lu *et al.*, *Science* **329**, 659 (2010).
 [16] L. A. Wray, S.-Y. Xu, Y. Xia, D. Hsieh, A. V. Fedorov, Y. S. Hor, R. J. Cava, A. Bansil, H. Lin, and M. Z. Hasan, *Nat. Phys.* **7**, 32 (2011).
 [17] S.-Y. Xu, M. Neupane, C. Liu, D. Zhang, A. Richardella, L. Andrew Wray, N. Alidoust, M. Leandersson, T. Balasubramanian *et al.*, *Nat. Phys.* **8**, 616 (2012).
 [18] A. M. Black-Schaffer, A. V. Balatsky, and J. Fransson, *Phys. Rev. B* **91**, 201411 (2015).
 [19] M.-X. Deng, M. Zhong, S.-H. Zheng, J.-M. Qiu, M. Yang, and R.-Q. Wang, *J. Appl. Phys.* **119**, 073903 (2016).
 [20] C. Timm, *Phys. Rev. B* **86**, 155456 (2012).
 [21] G. J. Ferreira and D. Loss, *Phys. Rev. Lett.* **111**, 106802 (2013).
 [22] C. Ertler, M. Raith, and J. Fabian, *Phys. Rev. B* **89**, 075432 (2014).
 [23] K. Nomura and D. Kurebayashi, *Phys. Rev. Lett.* **115**, 127201 (2015).
 [24] A. Pieper and H. Fehske, *Phys. Rev. B* **93**, 035123 (2016).
 [25] D.-X. Qu, Y. S. Hor, J. Xiong, R. J. Cava, and N. P. Ong, *Science* **329**, 821 (2010).
 [26] N. Nagaosa, J. Sinova, S. Onoda, A. H. MacDonald, and N. P. Ong, *Rev. Mod. Phys.* **82**, 1539 (2010).
 [27] D. Xiao, M.-C. Chang, and Q. Niu, *Rev. Mod. Phys.* **82**, 1959 (2010).
 [28] V. K. Dugaev, P. Bruno, M. Taillefumier, B. Canals, and C. Lacroix, *Phys. Rev. B* **71**, 224423 (2005).
 [29] N. A. Sinitsyn, J. E. Hill, H. Min, J. Sinova, and A. H. MacDonald, *Phys. Rev. Lett.* **97**, 106804 (2006).
 [30] E. J. Nicol and J. P. Carbotte, *Phys. Rev. B* **77**, 155409 (2008).
 [31] D. Xiao, G.-B. Liu, W. Feng, X. Xu, and W. Yao, *Phys. Rev. Lett.* **108**, 196802 (2012).
 [32] Z. Li and J. P. Carbotte, *Phys. Rev. B* **86**, 205425 (2012).
 [33] H.-Z. Lu and S.-Q. Shen, *Phys. Rev. B* **88**, 081304 (2013).
 [34] M. Tahir, A. Manchon, and U. Schwingenschlögl, *Phys. Rev. B* **90**, 125438 (2014).
 [35] Y. L. Chen, J. G. Analytis, J.-H. Chu, Z. K. Liu, S.-K. Mo, X. L. Qi, H. J. Zhang, D. H. Lu, X. Dai, Z. Fang *et al.*, *Science* **325**, 178 (2009).
 [36] Y. Okada, C. Dhital, W. Zhou, E. D. Huemiller, H. Lin, S. Basak, A. Bansil, Y.-B. Huang, H. Ding, Z. Wang *et al.*, *Phys. Rev. Lett.* **106**, 206805 (2011).
 [37] Q. Liu, C.-X. Liu, C. Xu, X.-L. Qi, and S.-C. Zhang, *Phys. Rev. Lett.* **102**, 156603 (2009).
 [38] D. A. Abanin and D. A. Pesin, *Phys. Rev. Lett.* **106**, 136802 (2011).

- [39] J. H. Wilson, D. K. Efimkin, and V. M. Galitski, *Phys. Rev. B* **90**, 205432 (2014).
- [40] K. N. Okada, Y. Takahashi, M. Mogi, R. Yoshimi, A. Tsukazaki, K. S. Takahashi, N. Ogawa, M. Kawasaki, and Y. Tokura, [arXiv:1603.02113](https://arxiv.org/abs/1603.02113).
- [41] I. Lee, C. K. Kim, J. Lee, S. J. L. Billinge, R. Zhong, J. A. Schneeloch, T. Liu, T. Valla, J. M. Tranquada, G. Gu *et al.*, *Proc. Natl. Acad. Sci. U.S.A.* **112**, 1316 (2015).
- [42] G. D. Mahan, *Many-Particle Physics*, 3rd ed. (Plenum, New York, 1993).